

$O(a)$ improvement of lattice QCD with two flavors of Wilson quarks



Karl Jansen^a and Rainer Sommer^b

^a CERN, Theory Division
CH-1211 Genève 23, Switzerland

^b DESY-Zeuthen
Platanenallee 6, D-15738 Zeuthen

Abstract

We consider $O(a)$ improvement for two flavor lattice QCD. The improvement term in the action is computed non-perturbatively for a large range of the bare coupling. The position of the critical line and higher order lattice artifacts remaining after improvement are estimated. We also discuss the behavior of the HMC algorithm in our simulations.

1 Introduction

The lattice provides a regularization for QCD, which allows us to study also non-perturbative aspects of the theory from first principles. In order to implement a lattice regularization, a non-vanishing lattice spacing a has to be introduced. To achieve the goal of making contact with the physical world, it is then unavoidable that results obtained, e.g. by numerical simulations, have to be extrapolated to zero lattice spacing in order to reach the continuum limit. The rate with which the continuum limit can be approached will then depend on the amount of contamination of the results by lattice spacing effects.

A systematic approach to reduce discretization errors is Symanzik's improvement programme for on-shell quantities [1–5]. Applying this programme for Wilson fermions, it turns out that for cancelling the $O(a)$ effects it is sufficient to add only one new term into the action as suggested by Sheikholeslami and Wohlert [6]. The coefficient c_{sw} multiplying this term then has to be tuned in such a way that no $O(a)$ effects remain in on-shell quantities. In order to achieve this, it is necessary to determine c_{sw} non-perturbatively by imposing suitable so-called improvement conditions [7–10]. For a complete cancellation of all $O(a)$ effects, also the improvement of various composite fields have to be performed, which introduces a not too large number of additional improvement coefficients.

This programme was successfully applied in the quenched approximation and the effects of improvement have been verified [10–16]. Since systematic uncertainties caused by lattice artifacts are strongly suppressed in the complete $O(a)$ improved theory, it is expected that simulations can be done at larger lattice spacing, reducing in this way their cost substantially. This point of view should hold in particular if we switch from the quenched approximation to the full theory, including also the effects of N_f flavors of dynamical fermions. Since simulations with $N_f \neq 0$ are much more expensive than ones with $N_f = 0$, we expect especially in this situation a considerable gain from performing a non-perturbative $O(a)$ improvement. In this paper we therefore will initiate the non-perturbative computation of the improvement coefficients starting by determining c_{sw} for $N_f = 2$ dynamical flavors of Wilson fermions. A short account of our work has already appeared in [17].

We emphasize again that, although we expect to be able to accelerate the approach to the continuum limit by determining the improved theory, nevertheless the extrapolation to zero lattice spacing has to be performed. Indeed, our results discussed below indicate that higher order corrections can still be non-negligible.

2 Determination of c_{sw}

Our determination of c_{sw} closely follows [8,10]. In these references on-shell $O(a)$ improvement and the use of the Schrödinger functional in this context are also thoroughly explained. In order to make the present paper reasonably self-contained, we will intro-

duce the improvement condition explicitly and outline the computation of c_{sw} . Unexplained notation is taken over from [8,10].

2.1 $O(a)$ improved QCD

We start from Wilson's formulation of lattice QCD [18]. The action is the sum of the usual plaquette terms and the quark action

$$S_{\text{F}} = a^4 \sum_x \bar{\psi}(x)(D + m_0)\psi(x), \quad (2.1)$$

where a denotes the lattice spacing. The Wilson-Dirac operator,

$$D = \frac{1}{2} \{(\nabla_{\mu}^* + \nabla_{\mu})\gamma_{\mu} - a\nabla_{\mu}^*\nabla_{\mu}\}, \quad (2.2)$$

contains the lattice covariant forward and backward derivatives, ∇_{μ} and ∇_{μ}^* . Energy levels and on-shell matrix elements computed with this action approach their continuum limits with a rate that is asymptotically linear in the lattice spacing. These leading linear terms may be cancelled by adding one improvement term to the Wilson-Dirac operator (2.2):

$$D_{\text{impr}} = D + c_{\text{sw}} \frac{ia}{4} \sigma_{\mu\nu} \hat{F}_{\mu\nu}, \quad (2.3)$$

where $\hat{F}_{\mu\nu}$ is the standard discretization of the field strength tensor [8]. The coefficient $c_{\text{sw}}(g_0)$ is a function of the bare gauge coupling g_0 and, when it is properly chosen, it yields the on-shell $O(a)$ improved lattice action, which was first proposed by Sheikholeslami and Wohlert [6]¹.

When considering matrix elements of local operators, their improvement has to be discussed as well. Here, we only need the improved isovector axial current,

$$(A_{\text{I}})_{\mu}^a = A_{\mu}^a + ac_{\text{A}} \frac{1}{2} (\partial_{\mu}^* + \partial_{\mu}) P^a, \quad (2.4)$$

where

$$A_{\mu}^a(x) = \bar{\psi}(x) \gamma_{\mu} \gamma_5 \frac{\tau^a}{2} \psi(x), \quad (2.5)$$

$$P^a(x) = \bar{\psi}(x) \gamma_5 \frac{\tau^a}{2} \psi(x), \quad (2.6)$$

∂_{μ} and ∂_{μ}^* denote the standard forward and backward lattice derivative and the Pauli-matrices τ^a act on the flavor indices of the quark fields. The pseudo-scalar density P needs no $O(a)$ improvement term, whereas for the axial current one introduces c_{A} as another improvement coefficient. Current and density defined above are not renormalized, but their multiplicative renormalization is of no importance in the following. The

¹ For completeness we note that special care has to be taken, when massless renormalization schemes are used. This issue is discussed in ref. [8], but is not of immediate relevance here, where we want to perform a non-perturbative computation of $c_{\text{sw}}(g_0)$ for $N_{\text{f}} = 2$.

coefficients c_{sw} and c_A are functions of the bare coupling but do not depend on the quark mass. Their perturbative expansion is known to 1-loop accuracy [19,9], in particular

$$c_{\text{sw}} = 1 + c_{\text{sw}}^{(1)} g_0^2 + \mathcal{O}(g_0^4), \quad c_{\text{sw}}^{(1)} = 0.2659(1). \quad (2.7)$$

Non-perturbatively, c_{sw} and c_A can be computed by imposing suitable improvement conditions.

2.2 The improvement condition

The general idea for formulating an improvement condition to fix the $\mathcal{O}(a)$ counter-term in the action is that the $\mathcal{O}(a)$ terms violate chiral symmetry. Hence chiral Ward identities are violated at non-vanishing values of the lattice spacing. In particular, the unrenormalized PCAC relation

$$\frac{1}{2}(\partial_\mu + \partial_\mu^*) \langle (A_1)_\mu^a(x) \mathcal{O} \rangle = 2m \langle P^a(x) \mathcal{O} \rangle \quad (2.8)$$

contains an error term of order a in Wilson's original formulation, which is reduced to $\mathcal{O}(a^2)$ in the improved theory. Eq. (2.8) can be taken to define a bare current quark mass m . Depending on the details of the correlation functions, such as the choice of the kinematical variables \mathcal{O} , the position x and boundary conditions, one obtains different values of m . These differences are of order a in general and are reduced to $\mathcal{O}(a^2)$ by improvement. Requiring m to be exactly the same for three choices of the kinematical variables allows us to compute the improvement coefficients c_{sw} and c_A .

In more detail, we now consider the Schrödinger functional [20–22] with boundary conditions

$$U(x, k)|_{x_0=0} = \exp(aC_k), \quad C_k = \frac{i}{6L} \text{diag}(-\pi, 0, \pi) \quad (2.9)$$

$$U(x, k)|_{x_0=T} = \exp(aC'_k), \quad C'_k = \frac{i}{6L} \text{diag}(-5\pi, 2\pi, 3\pi) \quad (2.10)$$

for the gauge fields and boundary conditions for the quark fields as detailed in ref. [10] (taking $\theta = 0$). For \mathcal{O} we choose

$$\mathcal{O}^a = a^6 \sum_{\mathbf{y}, \mathbf{z}} \bar{\zeta}(\mathbf{y}) \gamma_5 \frac{\tau^a}{2} \zeta(\mathbf{z}), \quad (2.11)$$

where ζ ($\bar{\zeta}$) are the “boundary (anti) quark fields” [8] at time $x_0 = 0$. Similarly we use

$$\mathcal{O}'^a = a^6 \sum_{\mathbf{y}, \mathbf{z}} \bar{\zeta}'(\mathbf{y}) \gamma_5 \frac{\tau^a}{2} \zeta'(\mathbf{z}), \quad (2.12)$$

with the “boundary fields” at $x_0 = T$. Eq. (2.8) then leads us to consider the correlation functions

$$f_A(x_0) = -\frac{1}{3} \langle A_0^a(x) \mathcal{O}^a \rangle, \quad f_P(x_0) = -\frac{1}{3} \langle P^a(x) \mathcal{O}^a \rangle \quad (2.13)$$

$$f'_A(T - x_0) = +\frac{1}{3} \langle A_0^a(x) \mathcal{O}'^a \rangle, \quad f'_P(T - x_0) = -\frac{1}{3} \langle P^a(x) \mathcal{O}'^a \rangle, \quad (2.14)$$

and a current quark mass is given by

$$m(x_0) = r(x_0) + c_A s(x_0), \quad (2.15)$$

where

$$r(x_0) = \frac{1}{4}(\partial_0^* + \partial_0)f_A(x_0)/f_P(x_0), \quad (2.16)$$

$$s(x_0) = \frac{1}{2}a\partial_0^*\partial_0 f_P(x_0)/f_P(x_0). \quad (2.17)$$

Another mass m' is similarly defined in terms of the primed correlation functions. Improvement conditions may be obtained, e.g. by requiring $m = m'$ for some choice of x_0 . In order to obtain an improvement condition that determines c_{sw} , it is, however, advantageous to first eliminate c_A , which is unknown at this point. To this end one observes that the combination

$$M(x_0, y_0) = m(x_0) - s(x_0)\frac{m(y_0) - m'(y_0)}{s(y_0) - s'(y_0)} \quad (2.18)$$

is independent of c_A , namely

$$M(x_0, y_0) = r(x_0) - s(x_0)\frac{r(y_0) - r'(y_0)}{s(y_0) - s'(y_0)}. \quad (2.19)$$

Furthermore, from eq. (2.18) one infers that M coincides with m up to a small correction of order a^2 (in the improved theory); M may hence be taken as an alternative definition of an unrenormalized current quark mass, the advantage being that we do not need to know c_A to be able to calculate it.

Now we define M' in the same way as M , with the obvious replacements. It follows that (amongst others) the difference

$$\Delta M = M(\frac{3}{4}T, \frac{1}{4}T) - M'(\frac{3}{4}T, \frac{1}{4}T) \quad (2.20)$$

must vanish, up to corrections of order a^2 , if c_{sw} has the proper value. This coefficient may hence be fixed by demanding

$$\Delta M = \Delta M^{(0)}. \quad (2.21)$$

Here $\Delta M^{(0)}$, the value of ΔM at tree-level of perturbation theory in the $O(a)$ improved theory, is chosen instead of zero, in order to cancel a small tree-level $O(a)$ effect in c_{sw} . In this way one ensures that the values for c_{sw} determined non-perturbatively approach exactly one when $g_0 \rightarrow 0$. To complete the specification of the improvement condition, we choose $L/a = 8, T = 2L$ and evaluate eq. (2.21) for quark mass zero, i.e. $M = 0$. (We use M without arguments to abbreviate $M(\frac{1}{2}T, \frac{1}{4}T)$ from now on, while ΔM as defined in eq. (2.20) refers to $x_0 = \frac{3}{4}T$.)

The small tree-level lattice artifact in eq. (2.21) is then evaluated to

$$a \Delta M^{(0)} \Big|_{M=0, c_{\text{sw}}=1} = 0.000277 \text{ at } L/a = 8. \quad (2.22)$$

Note that in the Schrödinger functional it is possible to set the quark mass to zero, since there is a gap in the spectrum of the Dirac operator of order $1/T$.

2.3 Numerical results for c_{sw}

For a range of bare couplings g_0 we want to solve eq. (2.21) for c_{sw} . The general numerical procedure (which was used in [10]) to achieve this is summarized as follows.

- i) For fixed parameters g_0 , c_{sw} and a few suitably chosen values of the bare quark mass, compute M and ΔM and interpolate linearly in M to find ΔM at $M = 0$.
- ii) At fixed g_0 , repeat i) for a few values of c_{sw} and find the value of c_{sw} that solves eq. (2.21) by a linear fit in c_{sw} .
- iii) Repeat i) and ii) for sufficiently many values of g_0 to be able to find a good approximant $c_{\text{sw}}(g_0)$ for the range of g_0 that is of interest.

Since we are now interested in the theory with two flavors of dynamical fermions, the calculation of M and ΔM for each choice of m_0, g_0, c_{sw} requires a separate Monte Carlo calculation. We did these calculations with the Hybrid Monte Carlo algorithm. Details of the simulations and our error analysis are discussed in Sect. 5. Here we note that these simulations are CPU-time intensive and it is therefore desirable to limit the number of simulations to be performed. We achieved this by a slight modification of i) and ii).

First of all, it was already found in the quenched approximation that ΔM is a very slowly varying function of M [10]. Only negligible errors (compared with the statistical ones) are introduced if one keeps M just close to zero, say $|aM| < 0.03$, instead of exactly zero. Of course, we must be careful when generalizing from the quenched approximation since there the quark mass enters only through the quark propagator (valence quark mass), while here the quark mass is present in the fermion determinant as well (sea quark mass). For one set of parameters c_{sw}, g_0 , we have therefore verified that also in the full theory ΔM depends only weakly on M . This is shown in Fig. 1. Note that g_0 is chosen relatively large, in order not to be in the situation where quark loops are trivially suppressed. Apart from this test, we have verified for each pair of c_{sw}, g_0 that the dependence of ΔM on the valence quark mass at fixed sea quark mass is much smaller than the statistical uncertainty of ΔM , even when the valence quark mass is increased to values of order $0.05/a$. From here on we therefore use ΔM for $|aM| < 0.03$ as estimates for ΔM at $M = 0$ rather than performing several runs and interpolating to $M = 0$. Note that most of our data for M , given in Table 1, are in fact much smaller than our bound $|aM| = 0.03$. Apart from the test just mentioned, we do of course always have valence and sea quarks with the same mass.

Next, let us discuss step ii). In particular, we want to show that it is not really necessary to perform calculations for several values of c_{sw} for *each* value of the bare coupling g_0 . Let us denote by $c_{\text{sw}}^{\text{impr}}(g_0)$, the desired value of c_{sw} for which the improvement condition is satisfied. For c_{sw} close to $c_{\text{sw}}^{\text{impr}}(g_0)$, ΔM will depend linearly on c_{sw} and the lattice artifact may be written as $\Delta M - \Delta M^{(0)} = \omega \cdot (c_{\text{sw}} - c_{\text{sw}}^{\text{impr}})$, with a slope $\omega(g_0)$ dependent on the gauge coupling. The numerical procedure adopted in [10] consists of fitting ΔM to this linear dependence separately for each value of the bare

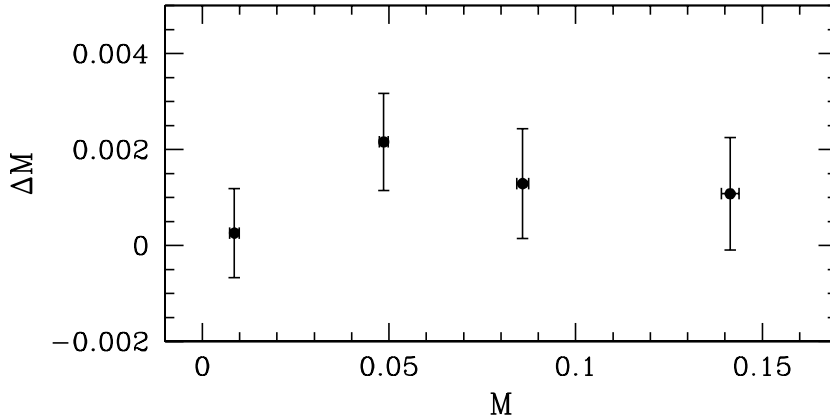


Figure 1: Mass dependence of the lattice artifact ΔM at $\beta = 6/g_0^2 = 5.4$, $c_{\text{sw}} = 1.7275$.

coupling g_0 . To improve on this, we may use the fact that the slope $\omega(g_0)$ is expected to be a smooth function of g_0 . Indeed, the numerical values of ω as determined in the quenched approximation show that $\omega(g_0)$ can well be described by a linear behavior in g_0^2 ,

$$\omega(g_0) = -0.015 \cdot (1 + \omega_1 g_0^2), \quad (2.23)$$

with a value of ω_1 small such that $\omega(g_0)$ does not differ much from the tree-level value $\omega(0) = -0.015$. This holds also for our results in full QCD as may be inferred from Table 1. It is therefore not necessary to determine ω for each value of g_0 separately. Instead, we use its smoothness to parametrize ω by an effective first order dependence on g_0^2 , and perform one global fit to all our data of ΔM of the form

$$a\Delta M - 0.000277 = \omega(g_0) \cdot (c_{\text{sw}} - c_{\text{sw}}^{\text{impr}}(g_0)). \quad (2.24)$$

The fit parameters here are ω_1 and the desired values $c_{\text{sw}}^{\text{impr}}(g_0^{(j)})$ at the different points $g_0^{(j)}$ where we have data. As an aside we remark that the fit to the $N_f = 2$ data, $\omega = -0.015 \cdot (1 - 0.33g_0^2)$, describes the slopes ω also for $N_f = 0$.

In this way, we obtain the values $c_{\text{sw}}^{\text{impr}}(g_0^{(j)})$ that satisfy our improvement condition. They are shown as data points in Fig. 2. In the whole range of g_0 , they are well parametrized by

$$c_{\text{sw}} = \frac{1 - 0.454g_0^2 - 0.175g_0^4 + 0.012g_0^6 + 0.045g_0^8}{1 - 0.720g_0^2}. \quad (2.25)$$

This representation, shown by the full curve in Fig. 2, is the main result of our work. It should be taken as a definition of the improved action for future work. In this way it is guaranteed that observables in the improved theory are smooth functions of the bare coupling and extrapolations to the continuum limit can be performed.

Table 1: Results for the current quark mass M and the lattice artifact ΔM .

β	κ	c_{sw}	aM	$a\Delta M$
12.0	0.12981	1.1329500	-0.0102(2)	-0.0007(2)
12.0	0.12981	1.1829500	-0.0031(1)	-0.0002(1)
12.0	0.12981	1.2329500	0.0038(1)	0.0004(1)
9.6	0.13135	1.2211007	-0.0031(2)	0.0000(1)
7.4	0.13460	1.2155946	-0.0008(5)	0.0017(3)
7.4	0.13396	1.2813360	0.0037(3)	-0.0001(3)
7.4	0.13340	1.3445066	0.0050(3)	-0.0002(4)
7.4	0.13245	1.4785602	-0.0002(5)	-0.0022(4)
6.8	0.13430	1.4251143	0.0014(4)	0.0000(3)
6.3	0.13500	1.5253469	0.0013(6)	-0.0004(4)
6.0	0.13910	1.2659000	0.0087(7)	0.0018(7)
6.0	0.13640	1.5159000	0.0025(7)	-0.0002(6)
6.0	0.13330	1.7659000	0.0108(5)	-0.0014(6)
5.7	0.14130	1.2798947	0.005(1)	0.0055(9)
5.7	0.13770	1.5569030	0.004(1)	0.0007(7)
5.7	0.13410	1.8339110	0.0045(6)	-0.0016(5)
5.4	0.14360	1.3571728	0.023(3)	0.004(4)
5.4	0.13790	1.7275432	0.009(1)	0.0003(9)
5.4	0.13250	2.0979135	0.007(2)	-0.0016(8)
5.2	0.13300	2.0200000	0.123(4)	-0.0006(9)

As in the quenched approximation, the $N_f = 2$ result is well approximated by perturbation theory (eq. (2.7)) for small couplings, say $g_0^2 \leq 0.5$. For larger couplings it grows quickly, although not quite as steeply as in the quenched approximation (the dashed curve).

An important issue is the question for which range of couplings eq. (2.25) is applicable. A priori it is to be trusted only for $\beta \geq 5.4$, where c_{sw} was computed by the numerical simulations. Extrapolations far out of this range are dangerous. We did, however, investigate whether it is justified to use eq. (2.25) at somewhat smaller β . Unfortunately, already for $\beta \approx 5.2$ the numerical simulations close to $M = 0$ turned out to be too time consuming for our 256 node APE-100 computer providing 6Gflop/s (sustained). What helps again is that ΔM hardly depends on M . Therefore we expect to find a small value of ΔM also at larger values of M , say $|aM| < 0.15$ (see Fig. 1), if the action is properly improved. Our calculation at $\beta = 5.2$ and $aM \approx 0.12$ yielded $a\Delta M = -0.0006(9)$, indicating that our improvement condition is indeed satisfied for

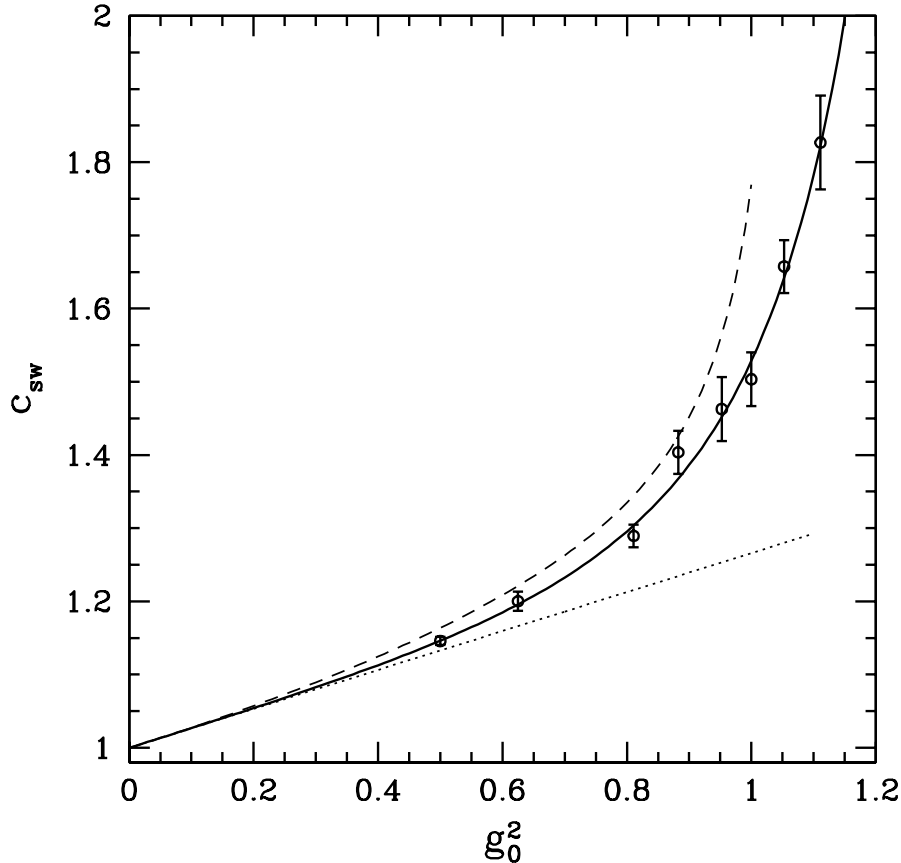


Figure 2: Non-perturbatively determined improvement coefficient c_{sw} for $N_f = 2$. The dotted line shows first order perturbation theory [19,9] and the dashed curve is the result for $N_f = 0$ [10].

c_{sw} as given by eq. (2.25) for β as low as $\beta = 5.2$. However, this calculation also revealed that higher order lattice artifacts rapidly become stronger when β is taken below $\beta = 5.4$. We will return to this issue in Sect. 4.

3 Estimate of κ_c

For future applications of the improved action, it is useful to roughly know the position of the critical line

$$\kappa = \kappa_c(g_0), \quad \kappa \equiv \frac{1}{2(am_0+4)}, \quad (3.1)$$

which is defined by the vanishing of the current quark mass. We will give an estimate for $\kappa_c(g_0)$ in this section. The critical line eq. (3.1) has an intrinsic uncertainty, since the position where the current quark mass vanishes depends on the very definition of the current quark mass. The uncertainty in the current quark mass is $O(a^2)$, translating

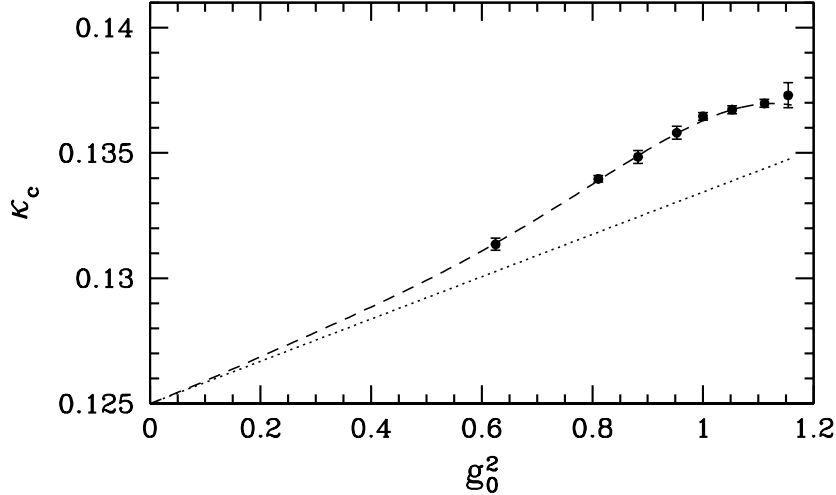


Figure 3: The critical line in the improved theory. The dashed curve gives the polynomial approximation to the non-perturbative result and the dotted line indicates first order perturbation theory.

into an $O(a^3)$ uncertainty in κ_c . From Fig. 9 in ref. [10], we estimate that the values of κ_c that one determines on a lattice with $L/a = 8$, might differ from κ_c determined on larger lattices by as much as 2×10^{-4} . This has to be kept in mind as an important limitation of the present determination of κ_c .

Our basis for an estimate of κ_c are the numerical data for M at a number of values of the parameters κ , g_0 , c_{sw} . For $\beta \geq 5.4$ the values of aM are rather small, see Table 1. One can convince oneself easily that it is justified in this case to use the 1-loop relations [23,24]:

$$M = Z_m m_q (1 + b a m_q), \quad a m_q = \frac{1}{2\kappa} - \frac{1}{2\kappa_c} \quad (3.2)$$

$$b = -1/2 - 0.0962 \cdot g_0^2, \quad Z_m = 1 + 0.0905 \cdot g_0^2, \quad (3.3)$$

to determine κ_c from κ , aM . The uncertainties due to left out higher order terms in the above equations may be neglected compared to the statistical uncertainties in M , since κ_c is close to κ in any case. As mentioned earlier, for $\beta = 5.4$, $c_{\text{sw}} = 1.7275$, we have a series of different values of κ . We have investigated whether the 1-loop relations describe $M(\kappa)$ in this case as well. Up to $aM \approx 0.14$ and within an error margin of about 5%, this is shown to be the case by our data. Therefore we also included the point $\beta = 5.2$, $aM \approx 0.12$ in the analysis – despite the relatively large mass of that point. The statistical uncertainties in aM are then translated into uncertainties in κ_c .

Next, we need to interpolate κ_c in c_{sw} to the proper values given by eq. (2.25). These are denoted by $c_{\text{sw}}^{\text{impr}}(g_0)$ below. In this interpolation, we use again that the slope

of κ_c as a function of c_{sw} is a smooth function of g_0 . We fit all values of κ_c to

$$\kappa_c = \kappa_c^{\text{impr}}(g_0) + k(g_0) \cdot (c_{\text{sw}} - c_{\text{sw}}^{\text{impr}}(g_0)), \quad (3.4)$$

$$k(g_0) = \sum_{i=1}^3 k_i(g_0)^{2i}. \quad (3.5)$$

Here, k_1 is set to its perturbative value of $-0.053/8$ [12], while k_2, k_3 and the desired values $\kappa_c^{\text{impr}}(g_0^{(j)})$ are fit parameters. Eq. (3.4) fits all values of κ_c within an error margin of $2 \cdot 10^{-4}$, which is also roughly the statistical accuracy of κ_c .

The results of the fit, $\kappa_c^{\text{impr}}(g_0)$, are shown as data points in Fig. 3. They are well approximated by the polynomial (dashed curve),

$$\kappa_c = 1/8 + \kappa_c^{(1)} g_0^2 + 0.0085 g_0^4 - 0.0272 g_0^6 + 0.0420 g_0^8 - 0.0204 g_0^{10}, \quad (3.6)$$

$$\kappa_c^{(1)} = 0.008439857. \quad (3.7)$$

The critical line is never very far from the 1-loop result $\kappa_c = 1/8 + \kappa_c^{(1)} g_0^2$ [25,19,9].

We emphasize once more that we regard eq. (3.6) as a first estimate and expect only a rather crude precision (statistical + systematic) of order $\pm 3 \cdot 10^{-4}$.

4 $O(a^2)$ effects after improvement

Once the improved action is known up to $O(a)$, a new question arises immediately: how large are higher order lattice artifacts after improvement? In the quenched approximation this has been investigated in the Schrödinger functional and also for low-energy hadronic observables [12,13,14,15,16]. Only rather small $O(a^2)$ effects have been found. In the full theory, such investigations will still take some time. Since our observable $M(x_0, T/4)$ should not depend on x_0 , apart from the $O(a^2)$ effects, it might serve meanwhile as estimator of the higher order lattice artifacts.

We plot $aM(x_0, T/4)$ and $aM'(x_0, T/4)$ in the lower part of Fig. 4, for $\beta = 5.4$ and a value of c_{sw} where ΔM almost vanishes as is obvious from the agreement between M and M' . Results for two values of κ are shown. They correspond to rather different M . At both values of M we observe that the variations of $aM(x_0, T/4)$ and $aM'(x_0, T/4)$ are within a corridor of ± 0.003 as long as $4a \leq x_0 \leq T - 4a$. As one takes x_0 closer to the boundaries, the values of M drop significantly below the values of M belonging to the corridor.

The middle part of the figure shows the situation for $\beta = 5.2$. Here, $x_0 = 4a$ is already outside of a corridor of the same size and $x_0 = 3a$ is quite far below. This indicates that at $\beta = 5.2$ the $O(a^2)$ lattice artifacts are already quite significant. Of course, their impact on quantities such as the hadron spectrum remains to be investigated in detail. Nevertheless, our analysis indicates that for values of β below $\beta = 5.2$, $O(a)$ improvement ceases to be very useful.

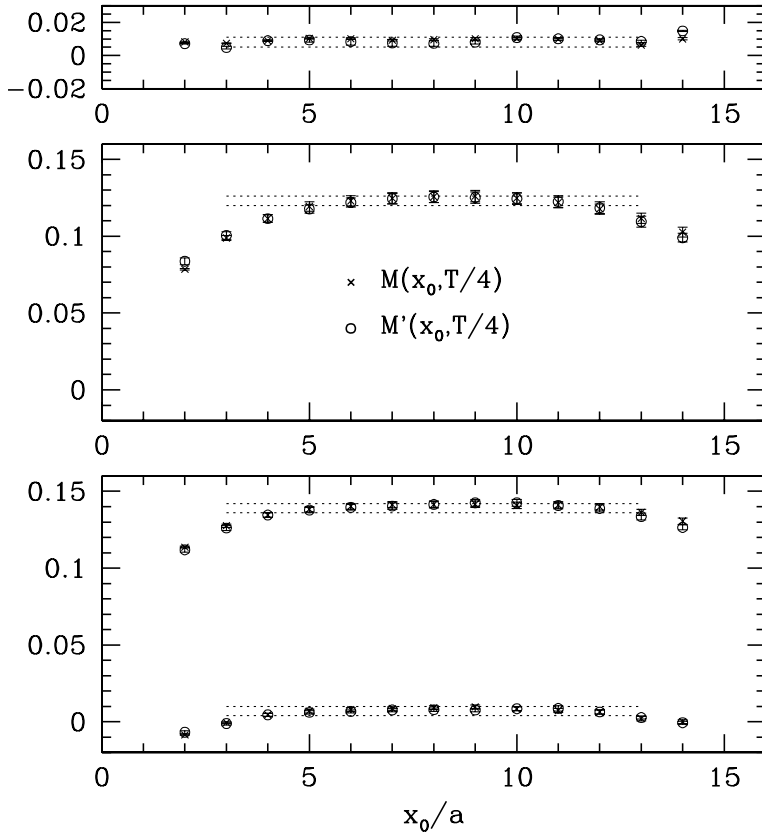


Figure 4: M and M' for $\beta = 5.4, c_{\text{sw}} = 1.7275$ (bottom part of the figure) and $\beta = 5.2, c_{\text{sw}}$ as given by eq. (2.25) (middle). The very top section is for $\beta = 6.0, c_{\text{sw}} = 1.8659, N_f = 0$. The time extent of the lattice is $T = 16a$.

The above conclusion is further strengthened by a comparison with the quenched approximation (top part of the figure) where – at a relatively large lattice spacing of $a \approx 0.1\text{fm}$ – the x_0 -dependence is hardly visible.

In interpreting the lattice artifacts in $M(x_0, T/4)$, one must be careful about the following point. Close to the boundaries, $x_0 = 0$ and $x_0 = T$, the spectral decomposition of the correlation functions, f, f' , receives noticeable contributions also from intermediate states with energies of the order of the cutoff. In such a kinematical regime, on-shell improvement is not applicable. We should therefore not put too much weight on the behavior very close to the boundaries. (For this reason we are not showing the points $x_0 = a$ and $x_0 = T - a$ in the figures.) Even with this reservation in mind, the difference between the quenched approximation at $a \approx 0.1\text{fm}$ and $N_f = 2$ QCD at $\beta = 5.2$ is striking.

We further note that preliminary results of the UKQCD collaboration [26] indicate that the lattice spacing is larger than 0.1fm at $\beta = 5.2, N_f = 2$. This is in line with the

considerable size of lattice artifacts visible in Fig. 4.

5 The Hybrid Monte Carlo simulation

In this section we want to present a number of aspects of the simulations we have performed. All numerical results quoted in this paper have been obtained by using the Hybrid Monte Carlo (HMC) algorithm [27]. One simulation (at $\beta = 6.8$) was repeated with the Polynomial Hybrid Monte Carlo algorithm [28,29], and completely consistent values were found for all observables compared [30].

Our particular implementation of the HMC algorithm using even/odd preconditioning [31] and including the improvement term of eq. (2.3) is described in detail in [32]. Throughout the simulations we used the higher order leap-frog integrator suggested in [33] to integrate the equations of motion to a trajectory length of one, implementing eq. (6.7) of ref. [33] with $n = 4$.

The program was run on the Alenia Quadrics (APE) massively parallel machine with 256 nodes. We decided to distribute our lattice of size $16 \cdot 8^3$ on these machines in such a way that we ran $N_{\text{rep}} = 32$ replica in parallel. These replica are independent copies of the lattice for identical choices of all parameters (apart from random numbers); we end up with N_{rep} statistically independent simulations for each set of parameters.

When starting our simulations, we tried to keep the acceptance rate to about 90%. However, it happened rather frequently that, despite this relatively large acceptance rate, in one of the replica a considerable number of trajectories in a row were rejected, inducing substantial autocorrelation times. Our solution to overcome this problem, was to perform every N_{safe} trajectories one with a much smaller step size, which we call the “safety step”. In principle, N_{safe} as well as the corresponding step size can be drawn randomly from arbitrary distributions, while still preserving detailed balance of the HMC algorithm. The choice of N_{safe} and the step size must, however, not depend on the Monte Carlo history. For simplicity we chose fixed values for N_{safe} and the step size before each run, determining reasonable values from our experience gained in simulations at other β 's and also during the thermalization phase.

We give in Table 2 the most relevant parameters of our simulations. By N_{traj} we denote the number of trajectories that equals the number of measurements per replicum. The strategy in performing the simulations was to start at a high value of $\beta = 12$ and then to decrease β successively to the values given in Table 2. We found, when changing from one β to the next smaller value, that only a short thermalization time of the order of ten trajectories was required.

5.1 Dynamics of the HMC – cost of a simulation

To achieve our physics goal, we performed quite a large number of simulations with different values of the parameters κ , β and c_{sw} . Although this was not our main objective, it is natural to also attempt to learn something about the dynamics of the algorithm.

Table 2: The parameters of the runs (we typically had $N_{\text{safe}} = 6$). We denote by $\delta\tau$ the step size of the leap-frog integrator, giving in brackets the value of the safety step size. P_{acc} denotes the acceptance rate and N_{CG} the average number of Conjugate Gradient iterations per inversion.

β	κ	c_{sw}	$\delta\tau(\delta\tau_{\text{save}})$	$N_{\text{traj}} \cdot N_{\text{rep}}$	P_{acc}	N_{CG}
12.0	0.12981	1.1329500	0.040	1600	0.976(3)	129.5(0.5)
12.0	0.12981	1.1829500	0.040	3264	0.981(2)	130.0(0.4)
12.0	0.12981	1.2329500	0.040	2080	0.978(3)	130.8(0.6)
9.6	0.13135	1.2211007	0.033	2304	0.985(3)	137.0(0.6)
7.4	0.13245	1.4785602	0.066(0.04)	1280	0.890(10)	138.3(1.3)
7.4	0.13460	1.2155946	0.066(0.04)	1632	0.902(10)	139.4(3.0)
7.4	0.13396	1.2813360	0.071(0.04)	3040	0.887(10)	133.8(0.2)
7.4	0.13340	1.3445066	0.033	1856	0.987(1)	154.9(0.7)
6.8	0.13430	1.4251143	0.066(0.025)	3104	0.859(12)	145.9(3.0)
6.3	0.13500	1.5253469	0.047(0.04)	1536	0.947(8)	165.2(1.3)
6.0	0.13330	1.7659000	0.033(0.02)	2080	0.958(6)	172.1(2.5)
6.0	0.13640	1.5159000	0.033(0.02)	2336	0.888(17)	186.2(4.5)
6.0	0.13910	1.2659000	0.033(0.02)	1856	0.966(3)	160.2(3.0)
5.7	0.14130	1.2798947	0.037(0.033)	1600	0.963(6)	168.7(3.0)
5.7	0.13410	1.8339110	0.040(0.033)	2528	0.920(10)	192.3(2.5)
5.7	0.13770	1.5569030	0.037(0.033)	2720	0.963(5)	179.5(2.0)
5.4	0.13790	1.7275432	0.033(0.027)	5120	0.948(8)	208.7(2.5)
5.4	0.14360	1.3571728	0.027(0.01)	3200	0.974(5)	205.6(1.4)
5.4	0.13250	2.0979135	0.027(0.01)	5760	0.958(7)	216.8(1.0)
5.2	0.13300	2.0200000	0.030(0.025)	3072	0.964(2)	163.3(1.1)

Before doing so, let us recall the special physical situation where these simulations were performed. We kept L/a and T/a fixed, and stayed close to the critical line. In contrast to the situation in infinite volume, the infrared cutoff is given by T and the quark mass, once small, plays only a minor role for the physics and hence also for the dynamics of the HMC algorithm. For the latter, a relevant quantity is the condition number,

$$k = \frac{\lambda_{\text{max}}}{\lambda_{\text{min}}}, \quad (5.1)$$

where λ_{min} (λ_{max}) are the lowest (largest) eigenvalues of the preconditioned matrix \hat{Q}^2 , see [32]. This quantity was computed in all simulations, using the method of ref. [34,35].

For quark mass zero and with Schrödinger functional boundary conditions, k has a value of order $(T/a)^2$ for free fermions [21]. In the interacting theory this is modified by terms of order g_0^2 . For the MC dynamics, the inverse square root of the condition

number is expected to roughly take over the role that the quark mass plays for infinite volume simulations.

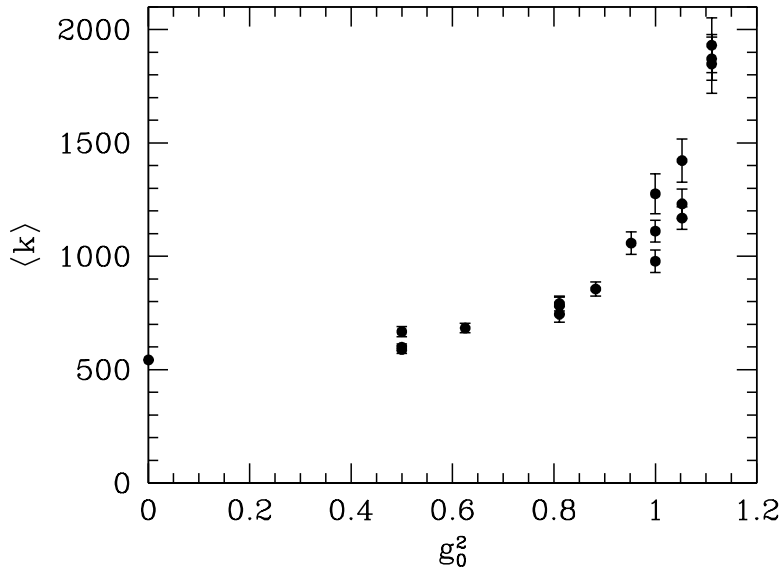


Figure 5: The expectation value of the condition number, eq.(5.1). When more than one value is plotted at a given value of g_0^2 they correspond to different values of c_{sw} . The tree-level value is shown at $g_0^2 = 0$.

In Fig. 5 we see a strong rise of $\langle k \rangle$ when g_0^2 is increased². For the largest values of the bare coupling, it is a factor three larger than the tree-level value at $g_0^2 = 0$. Of course, this is immediately reflected in a considerable rise in the number of CG iterations needed for the various “inversions” of \hat{Q}^2 . In fact, in our particular implementation of running N_{rep} simulations in parallel on a SIMD machine, there is an additional important overhead: the inversions have to run until the “slowest” replicum has converged. Therefore the number of CG iterations depends on the maximum of k over the number of replica, denoted by k_{max} . Since also the relative variance of k , defined by $\langle k^2 \rangle / \langle k \rangle^2 - 1$ grows from around 0.1 at $\beta = 12$ to 0.5 at $\beta = 5.4$, we find that $\langle k_{max} \rangle / \langle k \rangle$ can be as large as $\langle k_{max} \rangle / \langle k \rangle \approx 4$. We have not exactly quantified the corresponding loss in speed of the HMC as a function of N_{rep} , but expect that this may result in an overhead of 20-40% for $N_{rep} = 32$ ³.

In addition to its direct relation to N_{CG} , the condition number also is an important parameter, which has an influence on how large $\delta\tau$ may be chosen for a desired value of the acceptance P_{acc} . One may argue [36,37] that – for our leap-frog integrator – P_{acc} is approximately a universal function of the combination $y = (\delta\tau)^2 \langle k^{3/2} \rangle$. We observe

²The average is the usual ensemble average.

³ We remark that the condition number also develops a significant dependence on the quark mass when β becomes small and/or large quark masses are considered. For example at $\beta = 5.4$, $c_{sw} = 1.7275$ we find $\langle k \rangle = 1871(95)$ at $M = 0.009(1)$ whereas $\langle k \rangle = 800(14)$ at $M = 0.086(2)$.

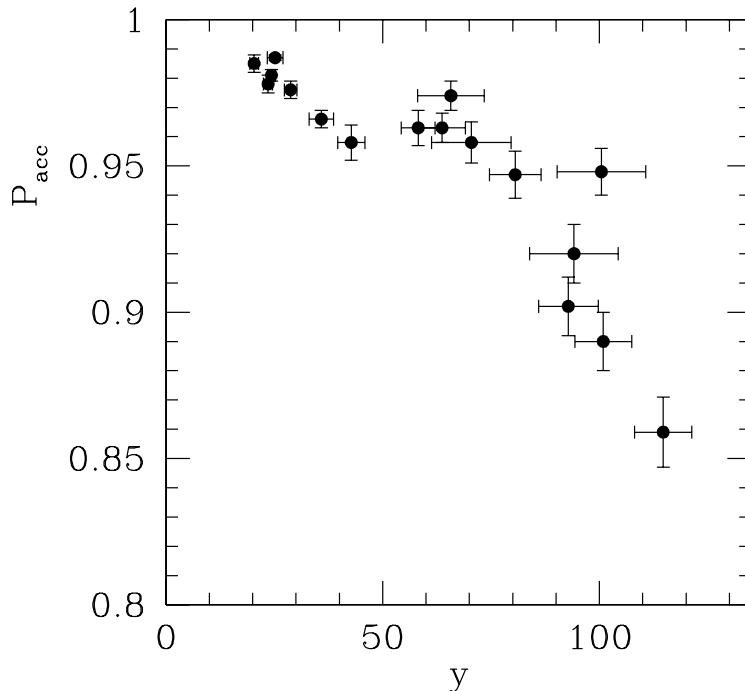


Figure 6: The acceptance rate as a function of $y = \delta\tau^2 \langle k^3/2 \rangle$. Only data with $|aM| < 0.03$ are included.

a rough consistency with such a scaling law (cf. Fig. 6).

As already mentioned earlier, the combination of the above effects leads to a large increase in the cost of the simulations when g_0^2 is increased. In the following section we will see that autocorrelations (mildly) enhance this effect further. This was one of the reasons why we did not decrease β below $\beta = 5.4$, where we invested already of the order of a month of CPU-time on our 6 Gflop/s (sustained) machine. Given that the length of our lattice might be around 2fm or larger for $\beta < 5.4$, it is in fact not a great surprise that simulations with very light quarks become difficult in this regime.

5.2 Error analysis and autocorrelation times

We used two different methods to obtain the errors of our observables. The first one is to average observables over all measurements done within one replicum. One is then left with $N_{\text{rep}} = 32$ statistically independent measurements. The errors, computed by jack-knife, then have no systematic uncertainty due to autocorrelations but they are only subject to a relative statistical uncertainty of $(2N_{\text{rep}})^{-1/2} = 12.5\%$.

Alternatively we performed a jack-knife procedure combined with the following blocking analysis. We generated an ensemble of blocked measurements by averaging (for each replicum) subsequent measurements over blocks of length L_{block} . The blocked measurements of different replica were joined to form one common sample (with $N_{\text{block}} =$

$N_{\text{rep}}N_{\text{traj}}/L_{\text{block}}$ blocks) from which we then computed the jack-knife error $\Delta(O)$ of the observable O . For large statistics, these errors will have a negligible statistical uncertainty, but still suffer from systematic corrections due to autocorrelations. For autocorrelation times τ , which are small with respect to L_{block} , the *systematic* effect due to autocorrelations is proportional to τ/L_{block} , while the relative *statistical* uncertainty of this error estimate is approximately given by $(2N_{\text{block}})^{-1/2}$. A typical situation is shown in Fig. 7 for the error of the lattice artifact ΔM . Since the autocorrelations for this quantity are not very large (see below), the error estimates converge quite well as $N_{\text{block}} \rightarrow N_{\text{rep}}$ ⁴. The most precise estimate of the true error of ΔM would probably be given by an extrapolation to $N_{\text{block}} = N_{\text{rep}}$ from larger values of N_{block} . On the other hand, there is a systematic (and subjective) bias in such an extrapolation and we prefer to quote the unbiased error estimate discussed before, which has a satisfactory statistical precision of 12.5% anyhow.

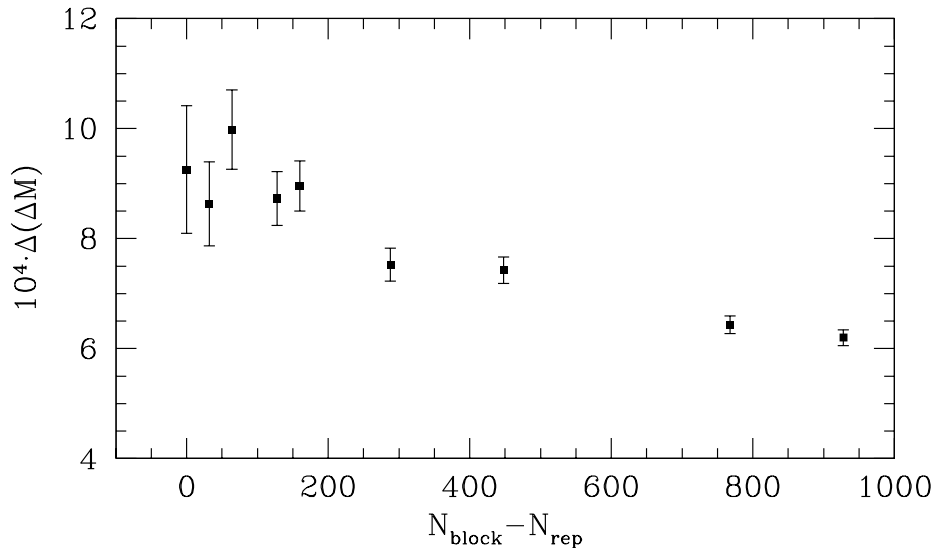


Figure 7: The error of the lattice artifact as a function of the number of blocks $N_{\text{block}} = N_{\text{rep}}N_{\text{traj}}/L_{\text{block}}$. The naive error is $\Delta_{\text{naive}} = 4.5 \cdot 10^{-4}$. The data are shown for parameters $\beta = 5.4$, $\kappa = 0.1379$, $c_{\text{sw}} = 1.7275432$.

Our definition of the integrated autocorrelation time τ_{int} of an observable O is

$$\tau_{\text{int}}(O) = \frac{1}{2} \left(\frac{\Delta(O)}{\Delta_{\text{naive}}(O)} \right)^2, \quad (5.2)$$

where Δ_{naive} is the naive error (computed with $L_{\text{block}} = 1$). Estimating the true error as described above, i.e. having $L_{\text{block}} = N_{\text{traj}}$, this quantity has a statistical uncertainty

⁴ We then have $L_{\text{block}} = N_{\text{traj}}$ and are back to the first method, where there is no systematic uncertainty of the error estimates. A little thought reveals that in general one expects an approximately linear behavior in $N_{\text{block}} - N_{\text{rep}}$ as suggested by Fig. 7.

of approximately $\Delta(\tau_{\text{int}}) = \sqrt{2/N_{\text{rep}}} \cdot \tau_{\text{int}}$. We show in Fig. 8 the integrated autocorrelation times for the lowest eigenvalue $\lambda_{\text{min}}(\hat{Q}^2)$ and for our main observable ΔM . The figure indicates that the autocorrelation times increase with growing bare coupling.

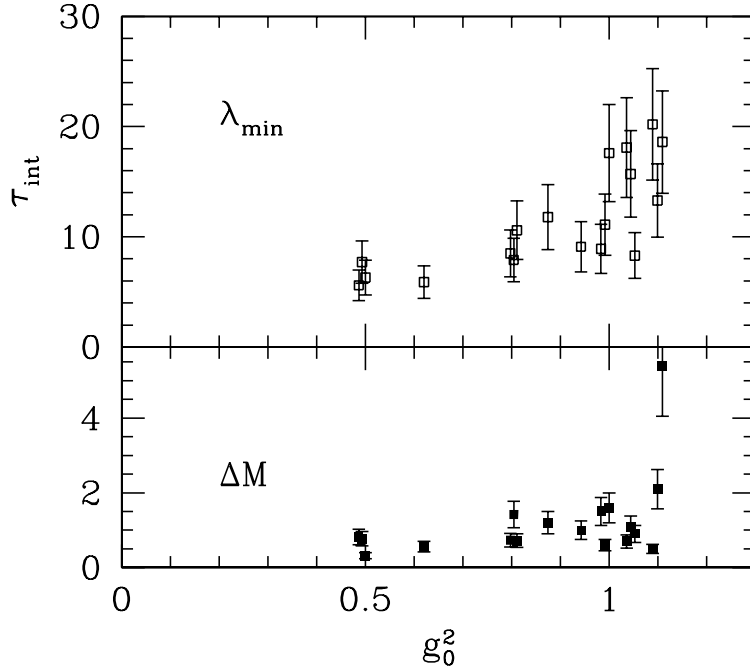


Figure 8: The integrated autocorrelation times of the lowest eigenvalue $\lambda_{\text{min}}(\hat{Q}^2)$ and the lattice artifact ΔM as a function of the bare coupling. When more than one value is plotted at a given value of g_0^2 , they correspond to different values of c_{sw} .

Furthermore, the integrated autocorrelation times depend strongly on the observable: for the lattice artifact ΔM , τ_{int} is always much below the one for $\lambda_{\text{min}}(\hat{Q}^2)$. We note that, on the contrary, the integrated autocorrelation times for the correlation functions f_A and f_P , from which ΔM is derived, are similar to the ones for $\lambda_{\text{min}}(\hat{Q}^2)$. Even larger autocorrelation times for other observables have been observed after cooling. As discussed in the following subsection, it is, however, very unlikely that they invalidate our error estimate for ΔM .

5.3 Metastable states

As an additional interesting observable we have also monitored the renormalized coupling constructed as described in [38] (with the derivative with respect to the background gauge field acting only on the pure gauge action). While for the larger values of β , this quantity showed autocorrelation times of the same order as $\tau_{\text{int}}(\Delta M)$, we observed a considerable rise in the integrated autocorrelation times eq.(5.2) for $\beta \leq 5.4$. We were worried that this behavior as well as the large values of $\tau_{\text{int}}(\lambda_{\text{min}})$ are due to difficulties

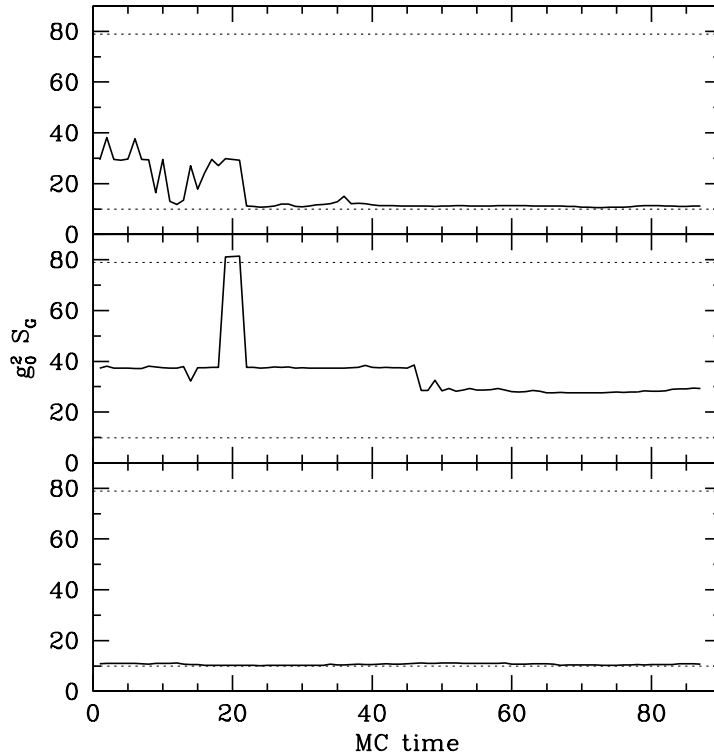


Figure 9: Part of the HMC history of the gauge field action S_G after cooling. We show three of our 32 replica. Simulation parameters are $\beta = 5.4, \kappa = 0.1325, c_{\text{sw}} = 2.0979$. The bounds (5.3) and (5.4) are shown as dotted lines.

of the HMC algorithm to sample different topological sectors as they have been observed before in large volume simulations [39] (see also [40]).

In order to investigate this possibility, we also examined the gauge fields after performing a number of cooling iterations [41], computing among other observables the gauge-field action and the topological charge Q (“naive definition”, see [42]). For our abelian background field, the gauge field action satisfies the bounds [20] (a small $O(a)$ correction is neglected here)

$$g_0^2 S_G \geq \pi^2, \quad Q = 0, \quad (5.3)$$

$$g_0^2 S_G \geq 8\pi^2 |Q|. \quad (5.4)$$

We note that eq. (5.4) is derived for smooth fields in the continuum Schrödinger functional, while eq. (5.3) is valid also for rough fields.

In all our runs where we performed cooling, we observed only once a value of Q different from zero. The short Monte Carlo (MC) time interval where this happened is contained in the MC history shown in the middle part of Fig. 9, where $g_0^2 S_G \approx 80$. Exactly during the interval where the action is above the limit eq. (5.4) with $|Q| = 1$, we

also observe that Q has an (approximately) unit value. Given their rareness, topological fluctuations appear not to be relevant in our small volume simulations and there is an indication that they are in fact not long-lived. In particular, slow *topological* fluctuations are clearly not the cause of the large autocorrelation times observed in our simulations.

Most of the time, the action (always after cooling in this section) is close to the absolute minimum of eq. (5.3). However, we also observed longer sections in the MC-history, where it remains at other values (e.g. $g_0^2 S_G \approx 40$). These appear to correspond to non-trivial local minima of the action (with $Q = 0$). Since these states are stable over several tens of trajectories, there is a mode with a very large autocorrelation time in the HMC simulations.

We now have to investigate whether our observable ΔM is affected by this large autocorrelation time, and the small τ_{int} determined in the previous section is misleading. We therefore want to know the correlation of ΔM with these states. As a measure of such a correlation we consider the linear correlation coefficient $\text{Cor}(\Delta M, g_0^2 S_G)$. A standard definition of the correlation coefficient of primary observables, a, b , (i.e. observables that are given directly as ensemble averages) is $\text{Cor}(a, b) = \text{Cov}(a, b) / [\text{Cov}(a, a)\text{Cov}(b, b)]^{1/2}$, where $\text{Cov}(a, b) = \langle (a - \langle a \rangle)(b - \langle b \rangle) \rangle$. Since we are mainly interested in ΔM , a derived quantity (i.e. a function of primary observables), we generalize the above definition to

$$\text{Cor}(a, b) = \left\{ \sigma^2(ab) - \langle b \rangle^2 \sigma^2(a) - \langle a \rangle^2 \sigma^2(b) \right\} / \left\{ 2 \langle a \rangle \langle b \rangle \sigma(a) \sigma(b) \right\} , \quad (5.5)$$

which can easily be used also for derived quantities, by computing the variances $\sigma^2(a)$ by a jack-knife analysis.

We found very small correlation coefficients between S_G and all fermionic observables considered, where of course the fermionic observables are the ones that enter the physics, i.e. they are computed without cooling. As an example we quote $\text{Cor}(\Delta M, g_0^2 S_G) = 0.02$ for $\beta = 5.4, c_{\text{sw}} = 2.0979$. We conclude that the metastable states that we observed are not a matter of major concern for our error analysis in the determination of c_{sw} .

This corroborates our error analysis of Sect. 5.2.

6 Conclusions

In this paper we have performed the first step to achieve a non-perturbatively $O(a)$ improved lattice theory for Wilson fermions. We have computed the improvement coefficient c_{sw} as a function of $\beta = 6/g_0^2$ in a range of couplings $\beta \geq 5.2$. This range of couplings seems to cover values of lattice spacings where simulations for e.g. studying hadronic properties can be performed. As our main result we consider the parametrization of eq. (2.25), which determines the non-perturbatively improved action for $N_f = 2$ dynamical flavors of Wilson fermions. A number of quantities such as the hadron spectrum can now be computed with lattice artifacts starting only at order a^2 and, indeed, such a programme has been initiated already [26]. In order to achieve the same accuracy

for hadronic matrix elements, also the improvement and normalization of the operators have to be determined along the lines exploited already in the quenched approximation [11,43,44] or following new suggestions [45].

Although after $O(a)$ improvement the linear lattice artifacts are cancelled, higher order discretization errors will remain. Indeed, we found indications that for $\beta < 5.4$ these effects can become significant. It would be desirable to investigate these effects further for additional physical observables.

During the course of our small volume simulations, we were also able to study the dynamical behavior of the Hybrid Monte Carlo algorithm used throughout this work. We found that the condition number of the fermion matrix rises with increasing coupling strength. The condition number directly influences various ingredients of the algorithm: changing β from large values to $\beta = 5.4$, we found that the number of Conjugate Gradient iterations increased by a factor of about 1.6, the step size had to be decreased by a factor of 2 and the autocorrelation times increased by about a factor of 2. All these effects add up to make simulations very expensive when β is chosen to be $\beta \approx 5.2$ or even smaller.

Acknowledgements

This work is part of the ALPHA-collaboration research programme. We thank DESY for allocating computer time on the APE/Quadrics computers at DESY-Zeuthen and the staff of the computer centre at Zeuthen for their support. We are grateful to Hartmut Wittig and Ulli Wolff for discussions and a critical reading of the manuscript. Martin Lüscher is thanked for numerous discussion and useful suggestions. We are thankful to Roberto Frezzotti for his help in comparing part of our results with those obtained with the PHMC algorithm.

References

- [1] K. Symanzik, Some topics in quantum field theory, in Mathematical problems in theoretical physics, eds. R. Schrader et al., Lecture Notes in Physics Vol. 153 (Springer, New York, 1982).
- [2] K. Symanzik, Nucl. Phys. B226 (1983) 187.
- [3] K. Symanzik, Nucl. Phys. B226 (1983) 205.
- [4] M. Lüscher and P. Weisz, Phys. Lett. 158B (1985) 250.
- [5] M. Lüscher and P. Weisz, Commun. Math. Phys. 97 (1985) 59.
- [6] B. Sheikholeslami and R. Wohlert, Nucl. Phys. B259 (1985) 572.
- [7] K. Jansen et al., Phys. Lett. B372 (1996) 275, hep-lat/9512009.
- [8] M. Lüscher et al., Nucl. Phys. B478 (1996) 365, hep-lat/9605038.

- [9] M. Lüscher and P. Weisz, Nucl. Phys. B479 (1996) 429, hep-lat/9606016.
- [10] M. Lüscher et al., Nucl. Phys. B491 (1997) 323, hep-lat/9609035.
- [11] M. Lüscher et al., Nucl. Phys. B491 (1997) 344, hep-lat/9611015.
- [12] M. Göckeler et al., Phys. Lett. B391 (1997) 388, hep-lat/9609008.
- [13] A. Cucchieri et al., (1997), hep-lat/9711040.
- [14] M. Göckeler et al., (1997), hep-lat/9707021.
- [15] H. Wittig, (1997), hep-lat/9710013.
- [16] R.G. Edwards, U.M. Heller and T.R. Klassen, (1997), hep-lat/9711052.
- [17] K. Jansen and R. Sommer, (1997), hep-lat/9709022.
- [18] K.G. Wilson, Phys. Rev. D10 (1974) 2445.
- [19] R. Wohlert, Improved continuum limit lattice action for quarks, DESY 87/069 .
- [20] M. Lüscher et al., Nucl. Phys. B384 (1992) 168, hep-lat/9207009.
- [21] S. Sint, Nucl. Phys. B421 (1994) 135, hep-lat/9312079.
- [22] S. Sint, Nucl. Phys. B451 (1995) 416, hep-lat/9504005.
- [23] S. Sint and P. Weisz, Nucl. Phys. B502 (1997) 251, hep-lat/9704001.
- [24] S. Sint, unpublished notes.
- [25] E. Gabrielli et al., Nucl. Phys. B362 (1991) 475.
- [26] UKQCD collaboration, private communication by H. Wittig.
- [27] S. Duane et al., Phys. Lett. B195 (1987) 216.
- [28] R. Frezzotti and K. Jansen, (1997), hep-lat/9709033.
- [29] R. Frezzotti and K. Jansen, Phys. Lett. B402 (1997) 328, hep-lat/9702016.
- [30] R. Frezzotti and K. Jansen, in preparation .
- [31] T.A. DeGrand and P. Rossi, Comput. Phys. Commun. 60 (1990) 211.
- [32] K. Jansen and C. Liu, Comput. Phys. Commun. 99 (1997) 221, hep-lat/9603008.
- [33] J.C. Sexton and D.H. Weingarten, Nucl. Phys. B380 (1992) 665.
- [34] B. Bunk et al., Conjugate gradient algorithm to compute the low-lying eigenvalues of the Dirac operator in lattice QCD, DESY internal report (September 1994).

- [35] T. Kalkreuter and H. Simma, *Comput. Phys. Commun.* 93 (1996) 33, hep-lat/9507023.
- [36] R. Gupta et al., *Phys. Rev. D*40 (1989) 2072.
- [37] S. Gupta et al., *Phys. Lett.* B242 (1990) 437.
- [38] M. Lüscher et al., *Nucl. Phys.* B413 (1994) 481, hep-lat/9309005.
- [39] B. Alles et al., *Phys. Lett.* B389 (1996) 107, hep-lat/9607049.
- [40] B. Alles et al., (1998), hep-lat/9803008.
- [41] M. Teper, *Phys. Lett.* 162B (1985) 357.
- [42] P.D. Vecchia et al., *Phys. Lett.* 108B (1982) 323.
- [43] M. Guagnelli and R. Sommer, (1997), hep-lat/9709088.
- [44] G.M. de Divitiis and R. Petronzio, (1997), hep-lat/9710071.
- [45] G. Martinelli et al., *Phys. Lett.* B411 (1997) 141, hep-lat/9705018.